International Journal of Nanotechnology and Applications
ISSN 0973-631X Volume 11, Number 3 (2017), pp. 265-276

http://www.ripublication.com

Synthesis, Characterization of Tin Oxide (SnO) Nanoparticles via Autoclave synthesis protocol for H_2 sensing

P.Durga Prasad, Siva Prasada Reddy, Adithya Deepthi, J.Prashanthi, G. Nageswara Rao*

School of chemistry, Andhra University, Visakhapatnam, A.P.-530003, India.

Abstract

The novel stannous oxide (SnO) nanoparticles were successfully synthesized by using the autoclave route at 120^{o}C, 150^{o}C, 180^{o}C & 200^{o}C and processed the 150^{o}C synthesized nanoparticles for 1hr, 2hrs, 3hrs & 4hrs. The crystalline phase, morphology and particle sizes had been characterized by X-ray diffraction (XRD), Scanning Electron Microscopy (SEM) and Energy dispersive X-ray spectroscopy (EDAX). The size of SnO nanoparticles was estimated by XRD pattern which revealed that SnO nanoparticles has tetragonal rutile phase except for the sample synthesized at 120^{o}C (which has orthorhombic structure). The chemical structural information of the synthesized nanoparticles was studied by Fourier transform infrared (FTIR) spectroscopy. The prominent UV emission peak was observed at 310nm in UV-spectra. The morphology of the SnO nanoparticles was observed from SEM images. SnO sensor material exhibited excellent sensitivity towards 500ppm of gas hydrogen gas at an operating temperature of 100^{o}C.

1. INTRODUCTION

A numerous nano based products has been developed by nanotechnology in many fields and are applied in many fields like electronics, textiles, cosmetics, pharmaceuticals, etc. The enhanced properties of nano materials has proven the potential impact on the environment and also raised the scientific and public concern towards the environment [(1)]. Nanoscale materials are essential ingredients for the development of functional materials, miniaturized devices, optoelectronics, biomedicine, catalysis, etc. Currently, there is a rising demand for nano-composite

based entities which exhibit reinforced properties and also demonstrate their applicability in diversified applications. Moreover, hybrid nano-composite materials are in present study of research in which two or more domains of selected metals, semiconductors, and/or oxides are interconnected through epitaxial bonding interfaces in highly structured configurations [(2)]. Nowadays, SnO has been regarded as a promising material for lithium ion rechargeable batteries because of its higher theoretical capacity (875 mA.h/g) compared to that of graphite (372 mA.h/g) as well as SnO_2 (783 mA.h/g) [(3)]. Numerous studies dealing with the physical, chemical and structural properties (including electronic and mechanical properties of tin oxides) on tin oxide have been reported [(4)].

The synthesis of nano metal oxides has been reported for their applications in various fields such as energy storage, magnetism, optics, catalysis, sensors, etc. Among several metal oxides, stannous oxide (SnO), controlling the shape and size at nano domain has exhibited a greater influence on their physiochemical properties [(6)]. Semiconductors of metal oxides have attracted much attention because of their potential applications in different fields of science and technology. Several simple metal oxide semiconductors have sufficient band gap energy for promoting or catalyzing a wide range of photochemical reactions of environmental interest [(7)]. A reduction in particle size to nanometer scale results in various interesting properties compared to the bulk properties. Stannous oxide (SnO), an important p-type semiconductor with direct optical band gap (Eg) of 2.5eV, has shown its significance in many fields of science and engineering and has been applied as coating substance, catalyst for the polymerization of lactic acids, thin film transistor TFT. SnO and other tin oxides are being used in different fields of technology, such as catalysis, chemical gas sensing, heat reflection and microelectronics.

Transparent conducting oxides (TCOs) are a class of materials that transmit visible radiation and conduct electricity. Tin oxide has also been one of the prominent materials in various industrial applications such as a transparent electrode, transparent thin film transistor, solar-electric energy conversion device and as a chemical sensor element [(5)]. The naturally formed tin (Sn) vacancies cause the variable direct band gap in SnO due to which this material has attracted considerable attention owing to its specific functional characteristics and significance in a various technological applications [(8)]. Noble metal nanostructures exhibit unusual optical properties because of the collective oscillations of charge density with optical frequencies, known as surface plasmons which have attracted considerable attention for potential applications in photonic devices and biosensors as well as medical imaging, diagnostics and therapeutics [(9)].

In present work we have synthesized SnO nanoparticles by autoclave route. SnO nanoparticles were synthesized at different temperatures as $120^{O}C$, $150^{O}C$, $180^{O}C$ and $200^{O}C$ respectively. Among the four samples, sample synthesized at $150^{O}C$ have

shown good results in XRD, EDAX, SEM characterizations.

2. EXPERIMENTAL:

Tin oxide (SnO) nanoparticles were synthesized under hydrothermal condition where stannous chloride ($SnCl_2.2H_2O$) and water (H_2O) were considered as precursor and solvent respectively. A calculated amount of $SnCl_2.2H_2O$ was added to 0.1M of HCl and transferred to volumetric flask to obtain homogenized solution (stock solution). This 100ml stock solution was then transferred to a teflon container of an autoclave, with addition of appropriate amount of urea. After sealing the autoclave, the autoclave was treated for 4hrs at different temperatures viz., 120^{o}C, 150^{o}C, 180^{o}C & 200^{o}C. After cooling, the powders were collected, centrifuged, air dried at room temperature and pulverized to obtain fine particles. Among these four samples, the SnO nanoparticles obtained at 150^{o}C has tetragonal structure which was confirmed by XRD and SEM. Hence re-synthesis of SnO nanoparticles at 150^{o}C was done and processed for 1hr, 2hrs, 3hrs & 4hrs in the autoclave. These samples also were extracted, centrifuged, air dried at room temperature and manually pulverized to obtain fine nanoparticles. The as synthesized samples of SnO were characterized to study their properties.

3. CHARACTERIZATION:

3.1 X-Ray Diffraction Studies (XRD):

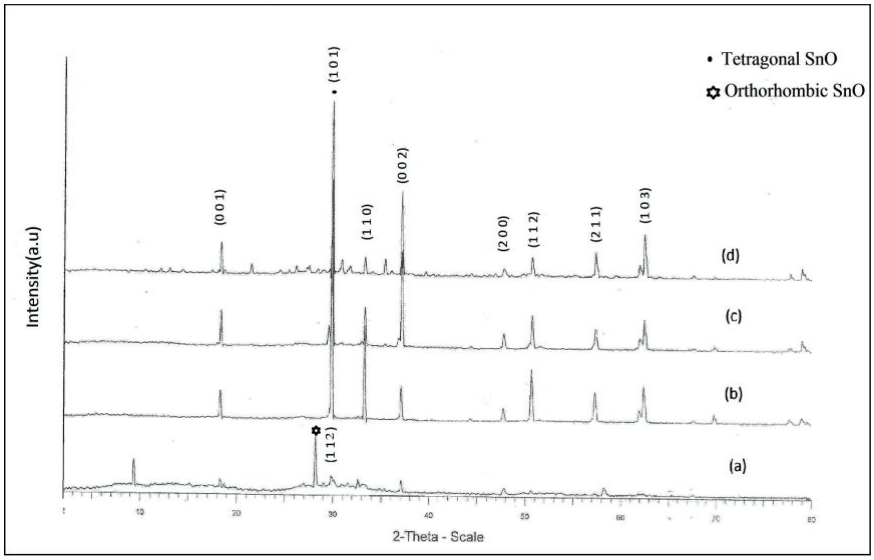

Fig 1. XRD pattern of SnO nanoparticles synthesize for 4hrs at (a) 120^{o}C (b) 150^{o}C (c) 180^{o}C & (d) 200^{o}C

The above figure shows the XRD patterns of SnO nanoparticles synthesized at different temperatures viz., 120^{o}C, 150^{o}C, 180^{o}C and 200^{o}C for 4hrs each. For 120^{o}C the peak is observed at 28.6^o corresponding to (1 1 2) plane by which the phase of the synthesized nanoparticles is confirmed to be orthorhombic from the JCPDS card no. 772296. The lattice parameters are observed as a=5A^o, b=5.7A^o, c=11.1A^o and lattice angles are observed as $\alpha=\beta=\gamma=90^o$. The crystallite size is calculated as whereas for the SnO nanoparticles synthesized at 150^{o}C, 180^{o}C & 200^{o}C, the peaks are observed at 18.2^o, 29.8^o, 33.2^o, 37.1^o, 44.3^o, 47.8^o, 50.7^o, 57.3^o, 62.0^o and 62.5^o corresponding to (0 0 1), (1 0 1), (1 1 0), (0 0 2), (2 0 0), (1 1 2), (2 1 1), (2 0 2) and (1 0 3) planes respectively by which the phase is found to be tetragonal from JCPDS card no. 060395. The lattice parameters are observed as a=3.8A^o, b=c=4.8A^o and lattice angles are observed as $\alpha=\beta=\gamma=90^o$. The average crystallite sizes are calculated as 12.95nm, 11.72nm, 10.43nm & 5.2nm for 120^{o}C, 150^{o}C, 180^{o}C & 200^{o}C for 4hrs respectively from which it can be inferred that the average crystallite size has been decreasing with the increase in synthesis temperature.

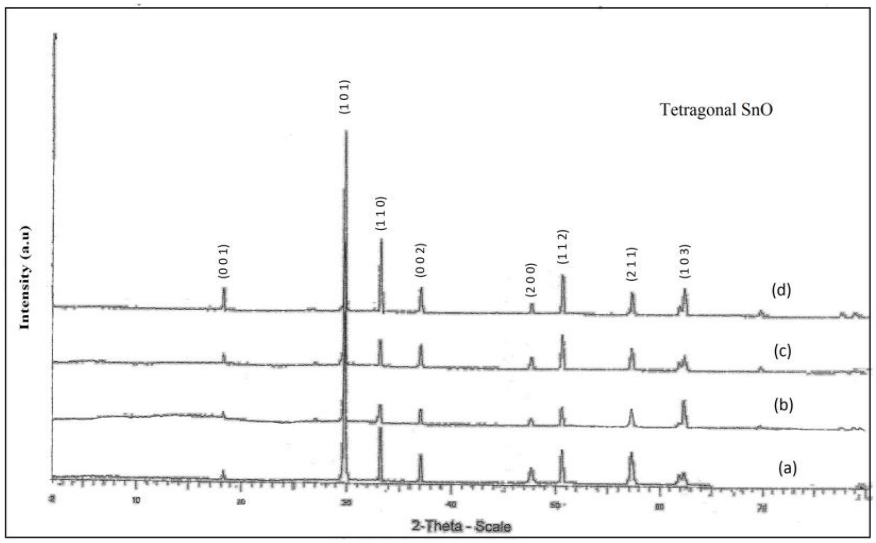

Fig. 2. XRD pattern of SnO nanoparticles synthesized at 150^{o}C for (a) 1hr (b) 2hrs (c) 3hrs & (d) 4hrs

Figure 2 shows the XRD pattern of SnO nanoparticles synthesized at 150^{o}C for different time durations viz., 1hr, 2hrs, 3hrs & 4hrs. For the SnO nanoparticles synthesized at 150^{o}C for 1hr, 2hrs, 3hrs & 4hrs, the peaks are observed at 18.2^o, 29.8^o, 33.2^o, 37.1^o, 44.3^o, 47.8^o, 50.7^o, 57.3^o, 62.0^o and 62.5^o corresponding to (0 0 1), (1 0 1), (1 1 0), (0 0 2), (2 0 0), (1 1 2), (2 1 1), (2 0 2) and (1 0 3) planes respectively by which the phase is found to be tetragonal from JCPDS card no. 060395. The lattice parameters are observed as a=3.8A^o, b=c=4.8A^o and lattice angles are observed as $\alpha=\beta=\gamma=90^o$. The crystallite sizes are calculated as 8.4nm, 9.02nm, 10.61nm &

11.72nm at 150^{o}C for 1hr, 2hrs, 3hrs & 4hrs respectively from which it can be inferred that the average crystallite size has been increasing with the increase in synthesis time. This might be due to the agglomeration of the particles with the increase in reaction time.

3.2 Fourier Transform Infra-Red Spectroscopy (FTIR):

For SnO nanoparticles synthesized at 120^{o}C, 150^{o}C, 180^{o}C & 200^{o}C, the absorption peaks are found at 3414cm^{-1} and 1629 cm^{-1} are attributed mainly to the O-H stretching vibration of surface hydroxyl group or adsorbed water of the SnO nanoparticles. The principal peak observed at 1586 cm^{-1} corresponds to the strong asymmetric stretching of C=O bond. The presence of N-O is confirmed from the peak observed at 1401 cm^{-1}. The absorption band at 526 cm^{-1} is ascribed to the terminal oxygen vibration of SnO which proved the significant presence of SnO material.

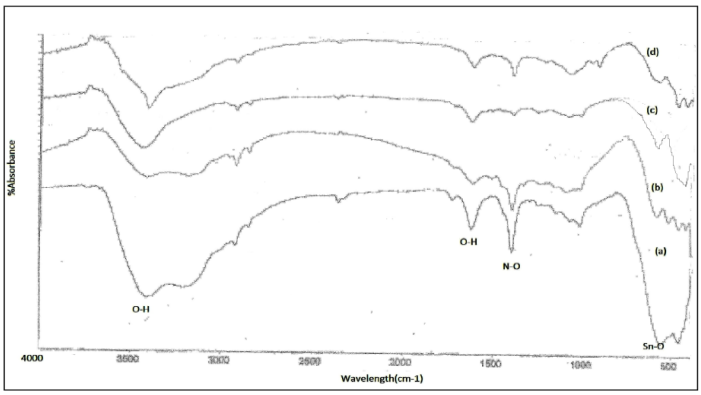

Fig.3. FTIR Spectra of SnO Nanoparticles Synthesized for 4 hrs at (a) 120^{o}C (b) 150^{o}C (c) 180^{o}C (d) 200^{o}C

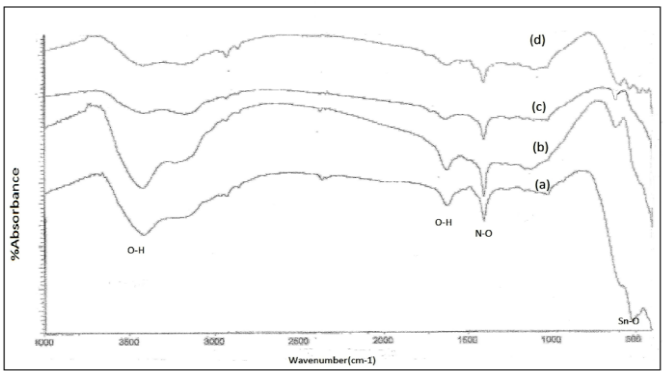

Fig. 4. FTIR pattern of SnO Nanoparticles Synthesized at 150^{o}C for (a) 1hr (b) 2 hrs (c) 3hrs (d) 4hrs

For SnO nanoparticles synthesized at 150ºC for 1hr, 2hrs, 3hrs and 4hrs, the absorption peaks are found at 3414cm^{-1} and 1629 cm^{-1} are attributed mainly to the O-H stretching vibration of surface hydroxyl group or adsorbed water of the SnO nanoparticles. The principal peak observed at 1586 cm^{-1} corresponds to the strong asymmetric stretching of C=O bond. The presence of N-O is confirmed from the peak observed at 1401 cm^{-1}. The absorption band at 516 cm^{-1} is ascribed to the terminal oxygen vibration of SnO which proved the significant presence of SnO material.

3.3 UV-Visible Diffusion Reflectance Spectroscopy (UV-DRS):

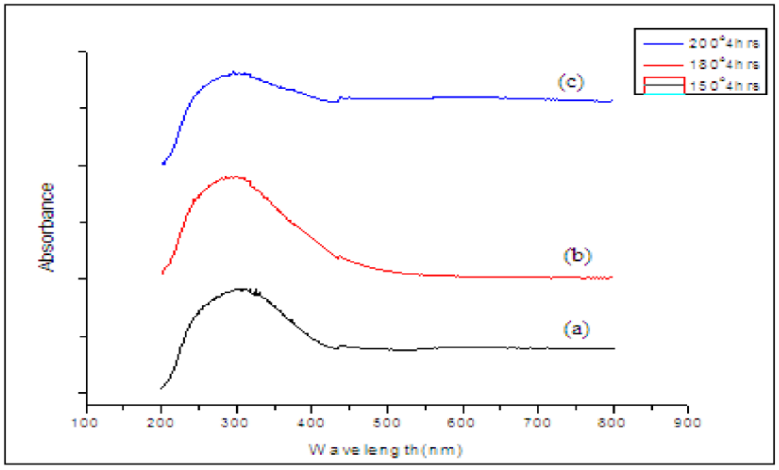

Fig.5. UV-DRS Spectra of SnO Nanoparticles Synthesized for 4 hrs at (a) 120ºC (b) 150ºC (c) 180ºC (d) 200ºC

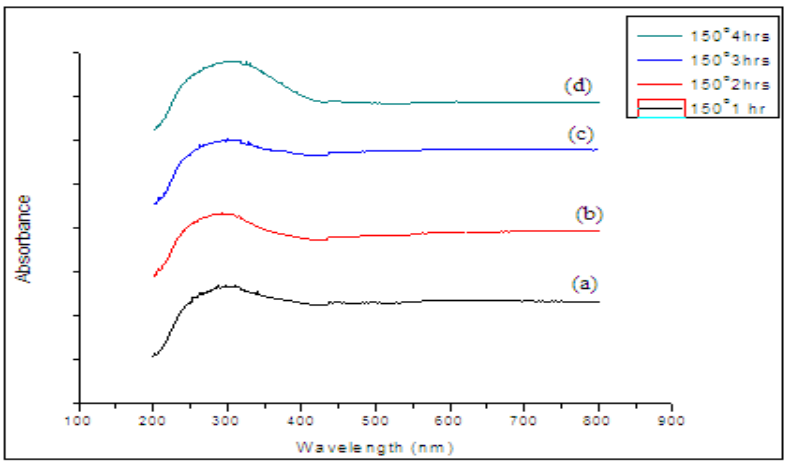

Fig.6. UV-DRS Spectra of SnO Nanoparticles Synthesized at 150ºC for (a) 1hr (b) 2 hrs (c) 3hrs (d) 4hrs

The maximum absorbances for SnO nanoparticles synthesized at 150^{o}C, 180^{o}C & 200^{o}C for 4hrs are observed at 310nm, 298nm & 292nm wavelengths from which the bandgaps are calculated as 4eV, 4.12eV & 4.25eV respectively. The maximum absorbance for SnO nanoparticles synthesized at 150^{o}C for 1hr, 2hrs, 3hrs & 4hrs are observed at 287nm, 292nm, 304nm & 310nm wavelengths from which the bandgaps are calculated as 4eV, 4.12eV & 4.25eV respectively. These calculated bandgaps are incoherence with the XRD results i.e., the bandgaps has been increasing with decrease in crystallite size and increase in synthesis temperature.

3.4 Scanning Electron Microscopy (SEM) & Energy Dispersive Analysis of X-Ray (EDAX):

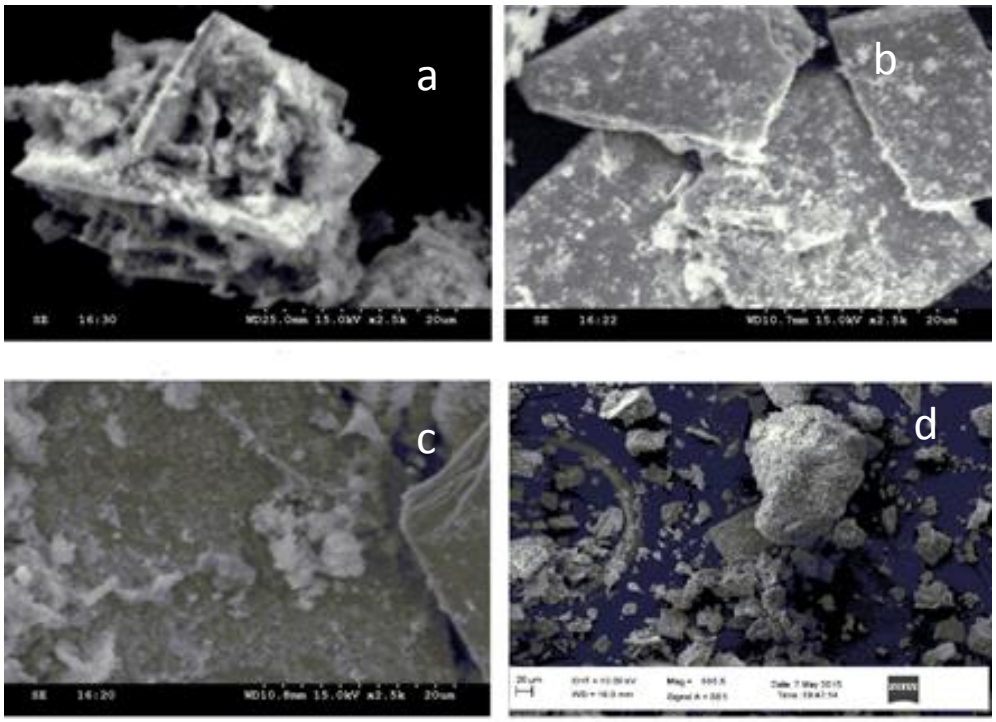

Fig.7. SEM micrographs of the SnO nanoparticles synthesized at (a) 120^{o}C, (b) 150^{o}C, (c) 180^{o}C & (d) 200^{o}C

From the above shown SEM images, it can be inferred that the synthesized SnO nanoparticles are crystalline in nature. The images 7 (a) & 7(b) clearly reveals the tetrahedral structure of the synthesized SnO nanoparticles. The sample synthesized at 200^{o}C has certain porosity which is shown in the figure 7 (d).

The above SEM micrographs clearly reveal the tetragonal structure of the synthesized SnO nanoparticles at different magnification parameters. The SnO nanoparticles

synthesized at 150^{o}C for 1hr exhibits significant porosity compared to that of SnO nanoparticles synthesized for 2hrs, 3hrs & 4hrs

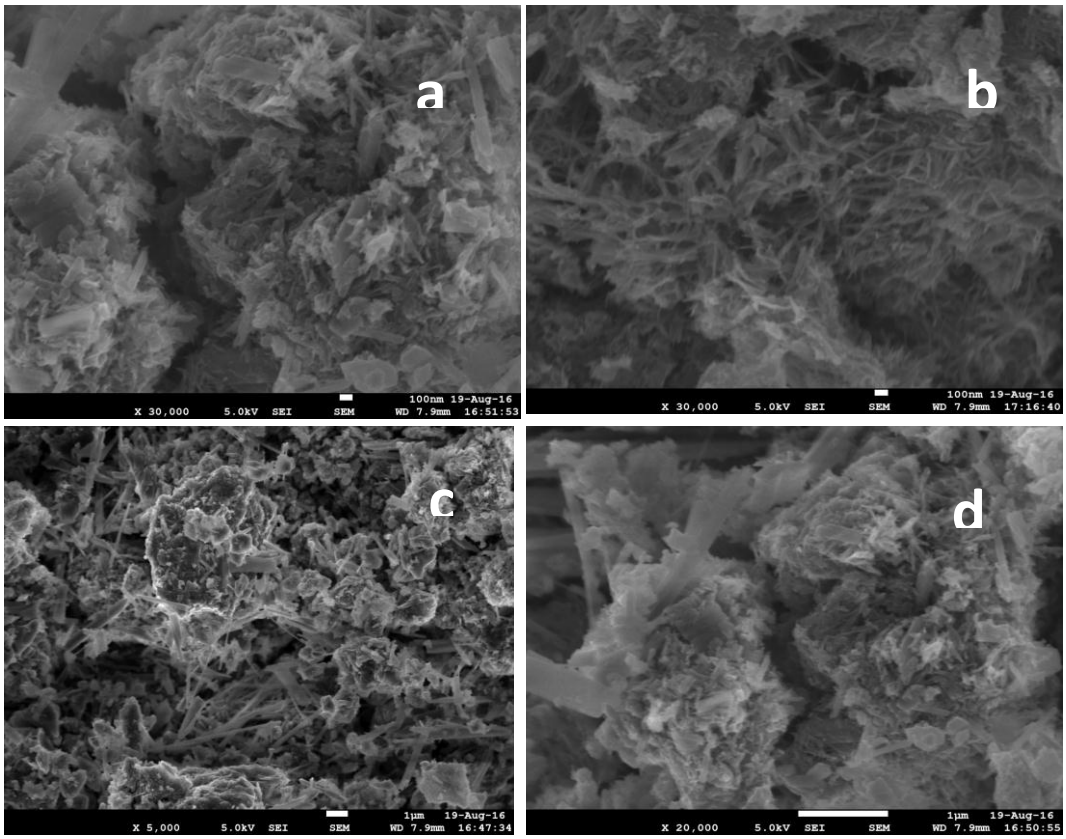

Fig.8. SEM micrographs of the SnO nanoparticles synthesized at 150^{o}C for (a) 1hr, (b) 2hrs, (c) 3hrs & (d) 4hrs

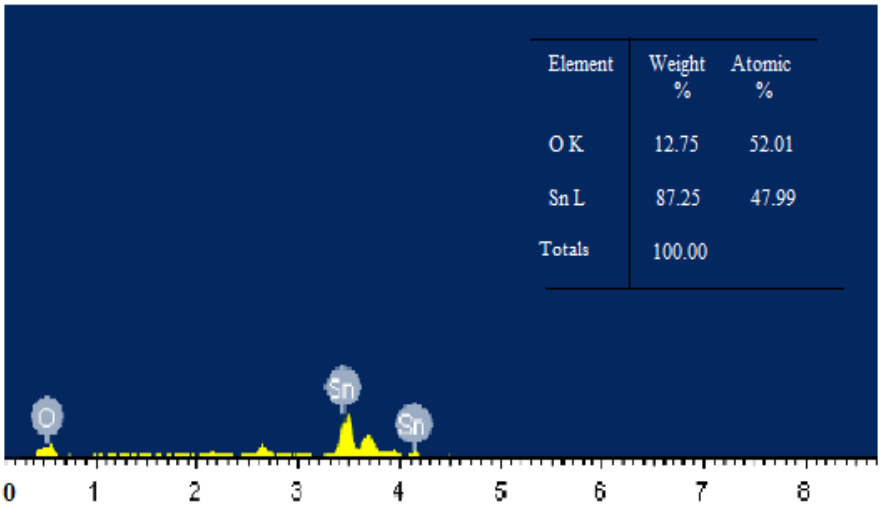

Fig.9. EDAX spectrum of SnO nanoparticles

From the above shown EDAX spectrum, it can be inferred that the sample contains 47.99 atomic percentage and 87.25 weight percentage of Sn; 52.01 atomic percentage and 12.75 weight percentage of oxygen which proved the desired elemental presence in the synthesized SnO nanoparticles.

4. GAS SENSING CHARACTERISTICS:

4.1 Fabrication of the sensor element

The substance used for the fabrication of the sensor element was alumina tube of 10 mm length, having two silver electrodes on either side separated by 6 mm; 5 mm external diameter and 3 mm internal diameter. For chemical sensor application, the sensor materials were mixed and ground with deionized water in an agate mortar to form a paste, then the resulting paste was coated on an alumina tube substrate having a pair of silver electrodes on either side followed by drying and calcination at 400^{o}C for 2h. Finally, a Ni-Cr heating wire is inserted into the tube to heat the sensor. The resulting sensor element, schematically shown in the inset of Fig. 10, was subjected to measurements of the electrical resistance in presence and absence of H_2 in air. A load resistor RL was connected in series with the sensor element Rs.

A chromel–alumel thermocouple (TC) was placed on the device to indicate the operating temperature. The operating temperature and concentrations of H_2 gas were varied in order to establish maximum sensor response.

The sensitivity (S) is defined as the ratio of change in conductance of the sensor exposed to the target gas to the original conductance of the medium.

$$S = Ra\text{-}Rg\ /Ra\ = \Delta R/Ra$$

Where Ra and Rg are the resistance of sensor in air and gas medium respectively.

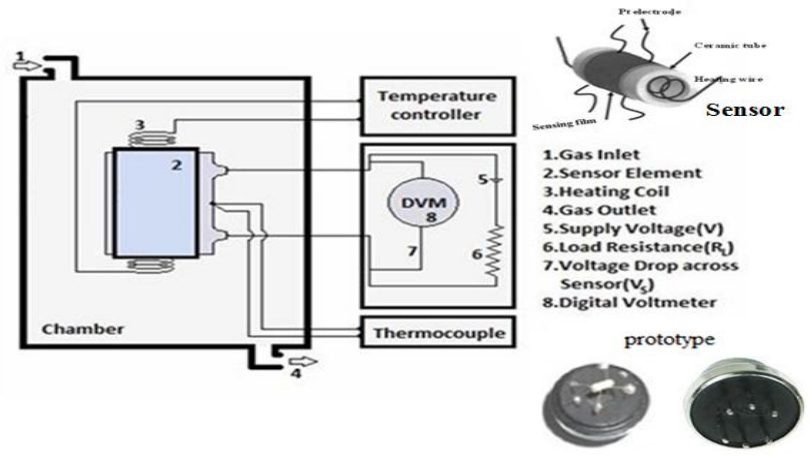

Fig.10 Schematic representation of gas sensor Measurement setup

The gas sensing properties of SnO nanoparticles was observed by performing gas sensing studies on sensor device. The sensitivity as a function of operating temperature towards 500ppm of H_2 gas is shown in figure 10. The sensor response increases with operating temperature and reaches maximum value at 100^{o}C followed by a decrease with increase in operating temperature. Optimization of operating temperature is crucial for establishing high sensitivity toward target gas. The response towards different gas concentrations of H_2 at 100^{o}C is shown in figure 10. The sensor showed high response of S= 0.23 towards 500ppm H_2 gas at comparatively low temperature i.e., 100^{o}C.

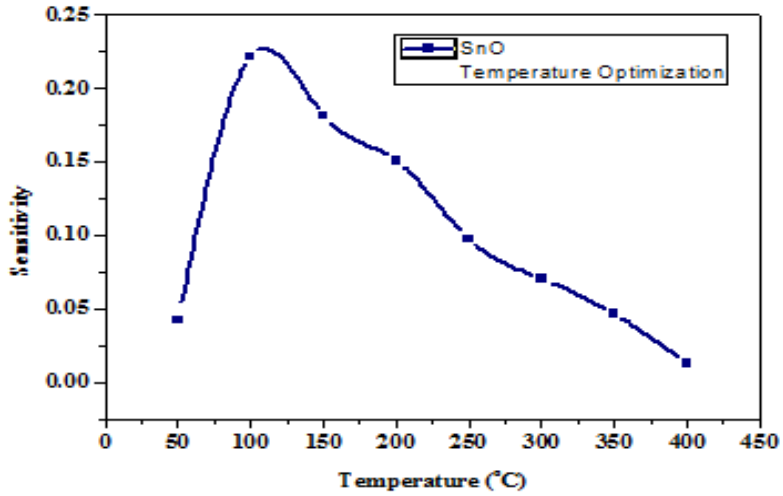

Fig.11. Gas sensing response of nano SnO

5. CONCLUSION:

Tin oxide (SnO) nanoparticles were synthesized by hydrothermal method varying temperature and synthesis time. Initially, the temperature was varied from 120^{o}C to 200^{o}C (120^{o}C, 150^{o}C, 180^{o}C & 200^{o}C) withstanding for 4hrs at each temperature. The other batch of synthesis was carried out at 150^{o}C by varying the time from 1hr to 4hrs (1hr, 2hrs, 3hrs & 4hrs). These samples were characterized by XRD, FTIR, UV-DRS, SEM & EDAX. From XRD results, the average crystallite size of the particles has been reducing with increase in synthesis temperature. FTIR results have revealed that the SnO nanoparticles synthesized at 150^{o}C for 1hr has the exact bond formation peak at 515cm^{-1} wave number when compared with the literature and a stable blue-black coloured SnO nanoparticles are formed with an average crystallite size of 8.4nm with perfect tetragonal crystal structure. The UV-DRS spectra have shown that the SnO nanoparticles synthesized at 150^{o}C for 1hr have high absorbance peak at comparatively minimum wavelength and the bandgap is calculated to be 4.3eV. Nano

SnO showed excellent sensitivity towards 500ppm H_2 gas at 100^{o}C. Hence, we conclude that the SnO nanoparticles synthesized at 150^{o}C for 1hr are best suitable for thinfilm based gas sensors.

REFERENCES:

[1] Pauline L. Waalewijn-Kool, Maria Diez Ortiz, Nico M. van Straalen, Cornelis A.M. van Gestel, Sorption, dissolution and pH determine the long-term equilibration and toxicity of coated and uncoated ZnO nanoparticles in soil, Environmental Pollution, 178, 59-64, 2013.

[2] Raffaella Buonsanti, Fabia Gozzo, Vincenzo Grillo, Mar Garcia-Hernandez, Elvio Carlino, Miguel Angel Garcia and P. Davide Cozzoli, Cinzia Giannini, Roberto Cingolani, Architectural Control of Seeded-Grown Magnetic-Semicondutor Iron Oxide-TiO Nanorod Heterostructures: The Role of Seeds in Topology Selection, J. Am. Chem. Soc. 132, 2437–2464, 2010.

[3] M. Zubair Iqbal, Fengping Wang, Rafi-ud-Din, M. Yasir Rafique, Qurat-ul-ain Javed, Asad Ullah, Hongmei Qiu, Synthesis of novel clinopinacoid structure of stannous oxide and hydrogen absorption characteristics, Materials Letters, 78, 50–53, 2012.

[4] Sanhita Majumdar, Shirshendu Chakraborty, P. Sujatha Devi, Amarnath Sen, Room temperature synthesis of nanocrystalline SnO through sonochemical route, Materials Letters, 62, 1249–1251, 2008.

[5] K.C. Sanal, M.K. Jayaraj, Growth and characterization of tin oxide thin films and fabrication of transparent p-SnO/n-ZnO p–n heterojunction, Materials Science and Engineering B 178, 816– 821, 2013.

[6] M. Zubair Iqbal, Fengping Wang, Rafi-ud-din, Qurat-ul-ain Javed, M. Yasir Rafique, Yan Li, Pengfei Li, Preparation, characterization and optical properties of tin monoxide micro-nanostructure via hydrothermal synthesis, Materials Letters 68, 409–412, 2012.

[7] Arun Kumar Sinha, Mukul Pradhan, Sougata Sarkar, and Tarasankar Pal, Large-Scale Solid-State Synthesis of Sn-SnO Nanoparticles from Layered SnO by Sunlight: a Material for Dye Degradation in Water by Photocatalytic Reaction, Environ. Sci. Technol. 47, 2339-2345, 2013.

[8] G. Vijayaprasath, G. Ravi & Y. Hayakawa, Effect of Solvents on Size and Morphologies of SnO Nanoparticles via Chemical Co-precipitation Method, International Journal of Science and Engineering Applications Special Issue NCRTAM, 2319-7560.

[9] Hong-Ying Fu, Xing-You Lang, Chao Hou, Zi Wen, Yong-Fu Zhu, Ming

Zhao, Jian-Chen Li, Wei-Tao Zheng, Yong-Bing Liu and Qing Jiang, Nanoporous Au/SnO/Ag heterogeneous films for ultrahigh and uniform surface-enhanced Raman scattering, J. Mater. Chem. C., 2, 7216–7222, 2014.